# Seawater ageing of thermoplastic acrylic hybrid matrix composites for marine applications

# Seawater Ageing of Thermoplastic Acrylic Hybrid Matrix Composites for Marine Applications

Machar Devine, Ankur Bajpai, Winifred Obande, Conchúr M. Ó Brádaigh, Dipa Ray*

School of Engineering, Institute for Materials and Processes, The University of Edinburgh, Sanderson Building, Robert Stevenson Road, Edinburgh, EH9 3FB, Scotland, United Kingdom.

*Corresponding author. *Email address*: dipa.roy@ed.ac.uk

Keywords:
A. Thermoplastic resin, B. Environmental degradation, B. Fibre/matrix bond, D. Mechanical testing, Water Ageing

## Abstract

Increasing usage of polymer composite materials necessitates the development of recyclable alternatives to traditional thermoset matrices or new techniques for recycling these materials. One family of promising recyclable matrices are the room temperature infusible acrylic resins, known commercially as Elium®. If these new materials are to be used in the tidal stream energy and shipping sectors, they must be able to withstand long-term immersion in seawater without significant losses in mechanical properties. In this study, accelerated seawater ageing is applied to acrylic/glass fibre and modified acrylic/glass fibre composites along with a traditional epoxy/glass fibre baseline. The mechanical properties (tensile, flexural, and short beam) are compared before and after ageing, and electron microscopy is used to examine fracture surfaces to determine the effects of water ingress on fracture propagation. In addition, the diffusion coefficients of the composites in seawater are compared and the changes in glass transition temperatures are used to determine the effects of plasticisation.

## 1 Introduction

The use of composite materials is rapidly growing, and as a result, so is the volume of composite waste. For example, it is estimated that onshore wind turbine blades alone will create over 43 million tonnes of composite waste by 2050 [1]. The usage of composites in marine sectors is also expected to grow to reach carbon neutrality targets; for example, the deployment of tidal stream turbines which use fibre-reinforced composite materials in their blades is required to expand fiftyfold [2], and decarbonisation of the shipping sector may include a switch to composite materials [3]. As these are generally large structures, they are currently manufactured with room-temperature infusible liquid thermoset resins via vacuum infusion.

Such thermoset composites are non-recyclable and are therefore disposed of in landfill or through incineration with the possibility of energy recovery, for example in cement kilns. It is therefore important to find recyclable alternatives that will allow increased production of large structures at room temperature and that perform equally well under seawater.

Traditional thermoplastic composites are not suitable for manufacturing very large structures, as they typically need the application of positive pressures (more than atmospheric vacuum) for the production of void-free laminates, due to their elevated melt viscosity and melting temperature. These positive pressures are normally applied by a press or autoclave, which is not economically feasible for very large structures such as ship sections and tidal energy blades [4]. Liquid acrylic resins (Elium®) from Arkema have the ease of processing of a thermoset resin (low viscosity at room temperature), but since they are thermoplastics, they can be recycled via crushing and heating [4], separation of the fibres and matrix through dissolution [5-7] or pyrolysis [8], or by thermoforming of the continuous fibre composite [5, 9]. The resins are largely composed of methyl-methacrylate monomers which are infused into reinforcement and polymerised in situ during composite manufacturing. Their room temperature processibility, low viscosity and promising mechanical properties [10] may make them a drop-in replacement for epoxy infusion resins.

A key consideration for the application of acrylic resins in the shipping and tidal sectors is their water absorption behaviour and retention of mechanical properties, even after a service life on the order of decades. The water ageing behaviour of acrylic composites reinforced with both glass fibres (GF) and carbon fibres (CF) has been reported by other researchers, but there is significant variation in the reported changes due to differences in materials, layup and ageing conditions. For example, Davies et al. [11] found that woven 0/90° GF/acrylic coupons exhibited a decrease in tensile modulus by 11% and tensile strength by 50% after 18 months of ageing in 60°C saltwater. The reported decreases in 0/90° CF/acrylic laminates, however, are smaller. Bel Haj Frej et al. [12] measured losses of 6% in tensile modulus and 10% in tensile strength of non-woven 0/90° CF/acrylic coupons after 6 months of ageing in distilled water at 70°C. Barbosa et al. [13] measured a decrease of only 4% in tensile modulus for woven 0/90° woven CF/acrylic coupons, and even a small increase of 3% in tensile strength, after ageing in distilled water at 80°C for 8 weeks. Consistently large reductions in short beam (shear) strength (SBS) have been measured

by several authors: Bel Haj Frej et al. [12] measured a 43% reduction in SBS for CF/acrylic composites and Nash et al. [3] saw a similar 38% reduction for GF/acrylic coupons.

Two main causes of degradation in mechanical properties of acrylic-matrix composites have been identified by several authors [3, 12-14] as swelling and plasticisation of the matrix and degradation of the fibre-matrix interface. The selection of matrix and reinforcement is therefore crucial to a composite's performance under water.

Acrylics are not considered high-performance matrices in structural composites. There is therefore an opportunity to improve their performance as composite matrices by hybridising them with other higher-performing engineering thermoplastics. Papers on a hybrid matrix of acrylic resin modified with polyphenylene ether (PPE) have already been published by the current researchers [15, 16]. These studies presented enhanced transverse flexural properties, initiation fracture toughness and solvent resistance of GF/acrylic-PPE composites compared to equivalent GF/acrylic composites, while retaining recyclability. This work is a continuation of the aforementioned work and investigates the seawater ageing behaviour of the GF/acrylic-PPE composites in comparison with GF/acrylic and an equivalent thermoset GF/epoxy composite. The diffusion of water in the composites is studied along with the drop in mechanical properties in the aged samples. The aged and dry samples are examined via scanning electron microscopy (SEM) to study the behaviour of the interface due to water ingress. The change in glass transition temperature due to seawater ageing is studied via dynamic mechanical analysis (DMA).

# 2 Materials and Methods

## 2.1 Manufacturing and Sample Preparation

Three types of unidirectional (UD) GF-reinforced laminates were manufactured: GF/acrylic, GF/acrylic-PPE and GF/epoxy. GF/acrylic laminates were made with an acrylic resin (Elium® 188 O, Arkema) and peroxide initiator (BP-50-FT, United Initiators) in a 100:3 ratio by weight. GF/acrylic-PPE laminates were made using 5 weight% of PPE oligomer with methacrylate end functionality (NORYL™ SA9000, SABIC) in the same acrylic resin, again with the BP-50-FT peroxide initiator in a 100:3 ratio. GF/epoxy laminates were prepared using SR 1710 Injection epoxy resin and SD 7820 hardener (Sicomin) in a 100:36 ratio by weight. The same unidirectional non-crimp E-glass fibre fabric (TEST2594-125-50,

Ahlstrom-Munksjö) with multi-compatible sizing was used for all matrix types, containing 600 g/m$^2$ of 0° fibres, 36 g/m$^2$ of 90° fibres and 10 g/m$^2$ of polyester stitching.

All laminates were prepared via a standard vacuum resin infusion route. Laminate thicknesses were 1.5 mm for tensile testing, 4 mm for flexural testing and SBS and 2 mm for diffusion coefficient measurement. After infusion, the laminates were left to polymerise at room temperature for 24 hours. The GF/epoxy laminates were then subject to a freestanding post-cure at 60°C for 8 hours followed by 100°C for 4 hours according to the manufacturer's recommendations. The GF/acrylic and GF/acrylic-PPE laminates did not require any post-cure.

## 2.2 Seawater Ageing

Composite specimens were subject to seawater ageing. Filtered natural seawater, collected from Gullane Beach in the Firth of Forth, Scotland, was maintained at 50°C and samples for mechanical testing were immersed for 3 months. Evaporated water was topped up with fresh water to maintain a constant water level. Aged specimens were kept immersed in seawater at room temperature until testing to prevent them from drying. Each of the mechanical tests detailed in the following sections was conducted on dry specimens as well as on aged specimens. In addition to specimens for mechanical testing, three nominally 160 × 160 × 2 mm specimens each of GF/acrylic, GF/acrylic-PPE and GF/epoxy were used to determine the diffusion coefficient and maximum water uptake. They were first oven-dried at 50°C for 5 days and then immersed in seawater at 50°C for 5 months. The specimens were removed from the water bath at 24-hour intervals, their surfaces were dried with a cloth and their weights were measured.

At each measurement interval, the percentage mass increase was calculated according to Equation 1 (ASTM D5229M) in which $M(t)$ is the percentage increase in mass caused by water uptake at time $t$, $W_i$ is the measured specimen mass at time $t$ and $W_o$ is the oven-dry specimen mass.

$$M(t) = \frac{W_i - W_o}{W_o} \times 100 \quad (1)$$

A Fickian diffusion curve of the form in Equation 2 (ASTM D5229M) where $h$ is the specimen thickness was then fitted, and values for the diffusion coefficient at 50°C ($D_z$) and equilibrium water content ($M_m$) were taken from the fitted curve.

$$M(t) = M_m \left\{1 - exp\left[-7.3\left(\frac{D_z t}{h^2}\right)^{0.75}\right]\right\} \quad (2)$$

## 2.3 Testing

### 2.3.1 Mechanical tests

Tensile testing (0° and 90°) was carried out according to ASTM D3039, using an MTS Criterion Model 45 300 kN test system. Specimens were spray-painted with a black and white speckle pattern to allow strain measurements to be taken with a video extensometer and the 0° tensile specimens were tabbed with an epoxy-glass composite. All tensile tests were conducted with a crosshead extension rate of 2 mm/min.

Flexural testing (0° and 90°) was carried out according to ASTM D7264 on an Instron 3369 test system using a span-to-thickness ratio of 32:1. The crosshead extension rate was set at 7 mm/min, and mid-span deflection was taken to be the crosshead extension. Short beam strength tests were performed in accordance with ASTM D2344, using a span-to-thickness ratio of 4:1. The crosshead extension rate was set at 1 mm/min.

### 2.3.2 Fibre Volume Fraction

Fibre volume fraction (FVF) and void fraction of the composites were measured using a matrix burn-off method according to ASTM D3171. The densities of the composite coupons, matrices and glass fibres were measured using a displacement method (ASTM D792).

### 2.3.3 Scanning Electron Microscopy

Scanning electron microscopy (SEM) was carried out using a JEOL JSM series microscope on fragments of 0° tensile specimens after fracture. Samples were sputter-coated with 30 nm of gold before imaging at 15 kV.

### 2.3.4 Dynamic Mechanical Analysis

The glass transition temperatures of both dry and aged specimens were measured using dynamic mechanical analysis (DMA). A TA Instruments Discovery DMA 850 was used in 3-point bend mode at a frequency of 1 Hz and an amplitude of 20 μm. Specimens were 50 × 13 × 1.5 mm with 0° fibres in the span direction. A ramp rate of 1 °C/min between ambient temperature and 180°C was selected and 1 specimen was tested for each composite type, both dry and saturated with water. Aged specimens were removed from the water bath, wiped to remove surface water and then immediately tested.

# 3 Results and Discussion

## 3.1 Water Absorption

A graph of percentage mass increase against the square root of time is presented in Figure 1. The experimental data as well as the fitted diffusion curves are shown in Figure 1 and the resulting $M_m$ and $D_z$ are given in Table 1. Each data point is the average increase of 3 specimens.

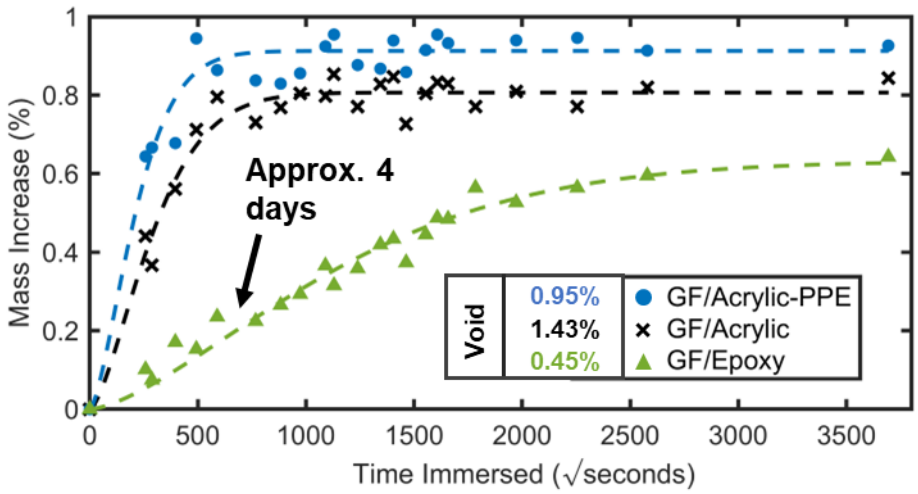


**Figure 1**

The GF/acrylic and GF/acrylic-PPE both exhibited Fickian behaviour—a linear increase in absorbed water when plotted against $\sqrt{t}$ which plateaus after reaching saturation (Figure 1). Although a Fickian diffusion curve is also fitted to the GF/epoxy data, there is a slight deviation from purely Fickian behaviour as there was an initial period of more rapid absorption followed by a more gradual mass increase after approximately 4 days (600 √s). The diffusion coefficients of GF/acrylic, GF/acrylic-PPE and GF/epoxy composites are given in Table 1 along with diffusion coefficient values of acrylic-matrix composites and unreinforced acrylic resin reported in published literature. The diffusion in GF/epoxy was an order of magnitude slower than in GF/acrylic and GF/acrylic-PPE.

These differences may be explained by considering the differences in structure and chemistry between the polymers and relating these to theories of diffusion. The structure of the acrylic matrix is typical of an amorphous thermoplastic and the epoxy has the typical structure of a thermoset. The structure of acrylic-PPE (5 weight% PPE), depicted in Figure 2 and Figure S1, has been previously investigated by Obande et

al. [15] and is believed to consist of PPE-rich cross-linked zones surrounded by acrylic-rich regions. The PPE with methacrylate end functionality reacts with the acrylic monomers during in-situ polymerisation to form crosslinks between acrylic chains.

**Table 1**

| **Material** | **Ageing Conditions** | $D_z$ **(×10$^{-12}$ m$^2$ s$^{-1}$)** | $M_m$ **(%)** | **Source** |
|---|---|---|---|---|
| GF/acrylic $[0°]_4$ | 50°C seawater 5 months | 1.81 | 0.81 | Current work |
| GF/acrylic-PPE $[0°]_4$ | 50°C seawater 5 months | 3.40 | 0.91 | Current work |
| GF/epoxy $[0°]_4$ | 50°C seawater 5 months | 0.15 | 0.63 | Current work |
| Acrylic/Carbon fibre | 70°C deionised water 6 months | 9.62/0.15* | 1.7/5.2* | [12] |
| PMMA Cast resin | 60°C deionised water | 4.54 | - | [17] |
| Acrylic (Elium 190) Cast resin | 60°C seawater 365 days | 4.23 | 1.90 | [14] |

*A dual Fickian model was fitted. Both diffusion coefficients and values for $M_m$ are presented.

Diffusion can be modelled using the free volume of the material, or by modelling the interaction between the polymer and the diffusant. In the *free volume theory*, the diffusant is assumed not to interact strongly with the material and instead diffuses through voids in the composite and the free volume in the matrix, to which the diffusion rate is highly sensitive [18, 19]. In the *polar interaction theory,* the diffusant forms bonds with polar sites in the polymer and water diffuses by hopping between these sites [18].

Free-volume diffusion is expected to occur in all three composites in this study, but the extent of free volume is likely to be less in GF/epoxy due to its 3D crosslinked network. Fujii et al. [20] demonstrated via quasi-elastic neutron scattering studies that the majority of water in PMMA is *free-water,* which occupies matrix free-volume and interacts little with the polymer. We expect similar behaviour in acrylic and acrylic-PPE matrix composites, shown schematically in Figures 2a(ii) and b(ii). Even if free-volume diffusion does not occur through the polymer, voids introduced by resin infusion and the presence of fibres also provide a route for water ingress. For example, in void-free epoxy, free-volume diffusion is not

expected to be significant, but free water content increases as more voids are introduced [21].

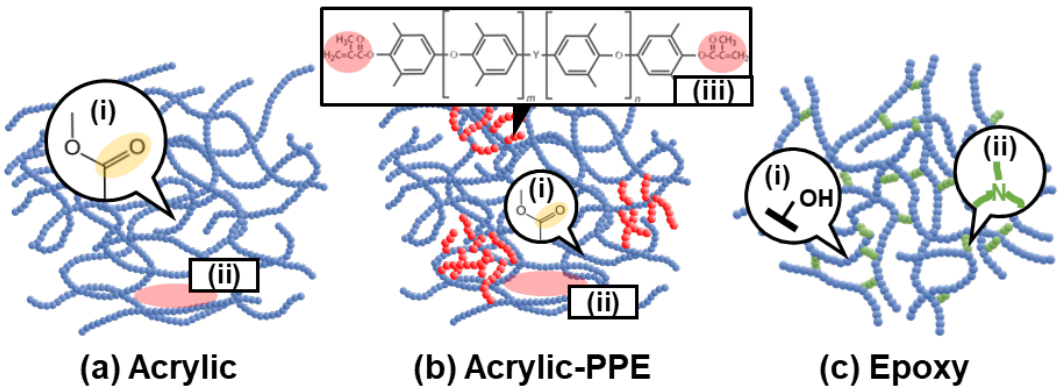


**Figure 2**

Additionally, polar interactions occur in all three matrices. In PMMA around 28% of water molecules exist as *intermediate water* [20] which interacts through hydrogen bonding with carbonyl groups on the PMMA side chains (Figures 2a(i) and b(i)). This interaction results in a slower motion of water molecules than in free water. In epoxy, water interacts with the hydroxyl groups attached to the polymer backbone and amine groups of the curing agents (Figure 2c) [22]. Epoxy/amine resins such as the Sicomin SR1710/SD7820 system used in this study are regarded as hydrophilic due to these groups, and hence the interaction with water is stronger than in PMMA.

In this study, GF/acrylic and GF/acrylic-PPE diffusion coupons both had higher void contents than the GF/epoxy, as displayed in Figure 1 and Table 2, which could explain the higher $D_z$ values of the thermoplastic composites. In addition to a higher void content, the acrylic matrices are thermoplastic amorphous polymers and are therefore likely to have more free volume than the crosslinked epoxy matrix [17, 22]. The GF/acrylic-PPE, however, shows a higher diffusion rate and final water content than the GF/acrylic, whereas the lower void fraction measured in the GF/acrylic-PPE would correspond to a lower diffusion rate under the free-volume theory. The differences in the polymer structure induced by the addition of PPE oligomers (Figure 2b) could increase the free volume and explain this observation. Considering the polar interaction theory, an increase in hydrophilicity is associated with slower diffusion [22, 23] and non-Fickian absorption behaviour, as noted in the GF/epoxy specimens in this study due to a mixture of free-volume and polar interaction diffusion [24, 25]. The stronger interaction between the

water and epoxy compared with the acrylic could therefore also contribute to the slower diffusion in GF/epoxy.

### 3.2 Dynamic Mechanical Analysis

DMA was used to determine the glass transition ($T_g$) of each composite specimen before and after ageing. Figure 3 presents the $T_g$ of each composite and the damping parameter (*tan δ*) vs temperature curves of each composite type from which the $T_g$ is derived. The reductions in $T_g$ indicate plasticisation of the matrices caused by the ingress of water [26, 27], which is associated with a decrease in matrix modulus and strength. Secondary peaks or shoulders in the *tan δ* curves of the aged specimens are observed in Figure 3 with the most prominent being in the case of GF/epoxy. This is attributed to drying of the specimens during DMA as observed in other studies [28]. After the drying peak, the *tan δ* curves closely follow the curves of the dry specimens.

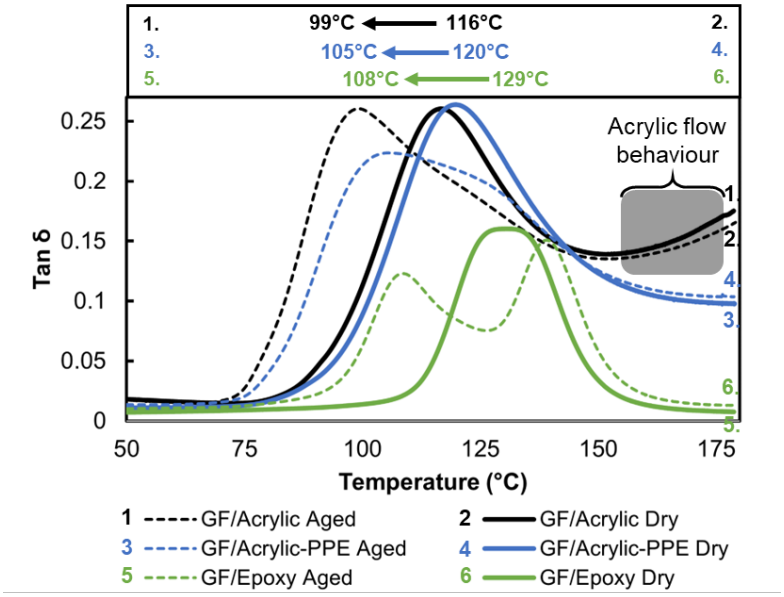


**Figure 3**

The addition of PPE resulted in enhanced thermomechanical properties. Firstly, the $T_g$ of GF/acrylic-PPE was 4°C higher than that of GF/acrylic when dry (120°C vs. 116°C), and 6°C higher when aged (105°C vs. 99°C). The GF/epoxy had a higher $T_g$ of 129°C when dry and 108°C when aged, as was expected due to its highly crosslinked structure. Secondly, there is a clear difference in behaviour between the acrylic and the acrylic-PPE composites at temperatures above the $T_g$ in Figure 3. A rise in *tan δ* after the $T_g$ peak is observed in GF/acrylic which is indicative of the beginning of flow behaviour, but this behaviour is absent in the GF/acrylic-PPE and the GF/epoxy. This difference in the behaviour of GF/acrylic-PPE is

due to the presence of intermittent crosslinked regions as depicted in Figure 2 and Figure S1. The suppression of flow behaviour through the addition of PPE may have implications in its use at high temperatures and in the fire safety of acrylic-PPE over acrylic, as melting and dripping of thermoplastics during a fire is a known safety hazard [29].

## 3.3 Mechanical Testing

Dry and aged specimens were tested in 0° and 90° tension, 0° and 90° flexure and for SBS. All 0° tensile and 0° flexural properties are normalised to 50% FVF. Representative stress-strain curves are available in Figures S2-S6.

### 3.3.1 Fibre and Void Volume Fractions

The densities of the acrylic, acrylic-PPE and epoxy matrices—as measured according to Section 2.3.2—used to calculate the fibre and void volume fractions were 1.18 g/cm$^3$, 1.15 g/cm$^3$, and 1.14 g/cm$^3$ respectively. The density of the glass fibres was similarly measured to be 2.60 g/cm$^3$. The fibre and void volume fractions of the laminates manufactured for each test are given in Table 2.

**Table 2**

| | Matrix | Fibre fraction (vol.%) | Void fraction (vol.%) |
|---|---|---|---|
| **Diffusion Specimens** | Acrylic | 56.8 ± 0.4 | 1.4 ± 0.1 |
| | Acrylic-PPE | 55.8 ± 0.3 | 1.0 ± 0.3 |
| | Epoxy | 52.8 ± 0.2 | 0.5 ± 0.1 |
| **90° Tension Specimens** | Acrylic | 53.5 ± 0.5 | 2.1 ± 0.3 |
| | Acrylic-PPE | 53.5 ± 0.3 | 0.8 ± 0.4 |
| | Epoxy | 50.9 ± 0.7 | 1.7 ± 0.5 |
| **0° Tension Specimens (Average of 2 Laminates)** | Acrylic | 53.5 ± 0.8 | 1.9 ± 0.8 |
| | Acrylic-PPE | 54.7 ± 0.8 | 1.9 ± 0.7 |
| | Epoxy | 49.0 ± 1.2 | 0.4 ± 0.3 |
| **0/90° Flexure, Short Beam Strength Specimens** | Acrylic | 56.4 ± 0.3 | 1.9 ± 0.4 |
| | Acrylic-PPE | 52.7 ± 0.2 | 1.9 ± 0.3 |
| | Epoxy | 54.6 ± 0.3 | 1.1 ± 0.1 |

### 3.3.2 Tension

As shown in Figure 4a, the 0° tensile moduli were not decreased by water ageing, and the marginal increases after ageing are considered within experimental error. The 0° modulus is dominated by the fibres which are not significantly affected by ageing; therefore, the moduli remain approximately

constant. In the dry specimens, the GF/epoxy had a 9% and 4% higher strength than GF/acrylic and GF/acrylic-PPE respectively. The decrease due to ageing is highest in GF/epoxy, however—21% versus 11% and 13% drops in GF/acrylic and GF/acrylic-PPE respectively (Figure 4b)—therefore the GF/epoxy has the lowest strength after ageing.

In contrast to 0° tension, there were drops in the 90° tensile modulus attributed to matrix plasticisation. The decrease in modulus was largest for GF/epoxy at 18%, nearly double the drop observed in the GF/acrylic and GF/acrylic-PPE (Figure 4c). Before ageing, the moduli of the three composites were approximately equal, but the larger decrease in GF/epoxy modulus meant that after ageing the GF/acrylic and GF/acrylic-PPE had 14% and 11% higher moduli respectively.

The 90° tensile strengths of the GF/acrylic and GF/acrylic-PPE were higher than GF/epoxy when both dry and aged. Water ageing caused only a small decrease in GF/acrylic strength of 4%, but the decreases in GF/acrylic-PPE and GF/epoxy were larger at 10% and 13% respectively (Figure 4d). After ageing, therefore, the GF/acrylic's strength was 16% higher than GF/epoxy and 10% higher than GF/acrylic-PPE.

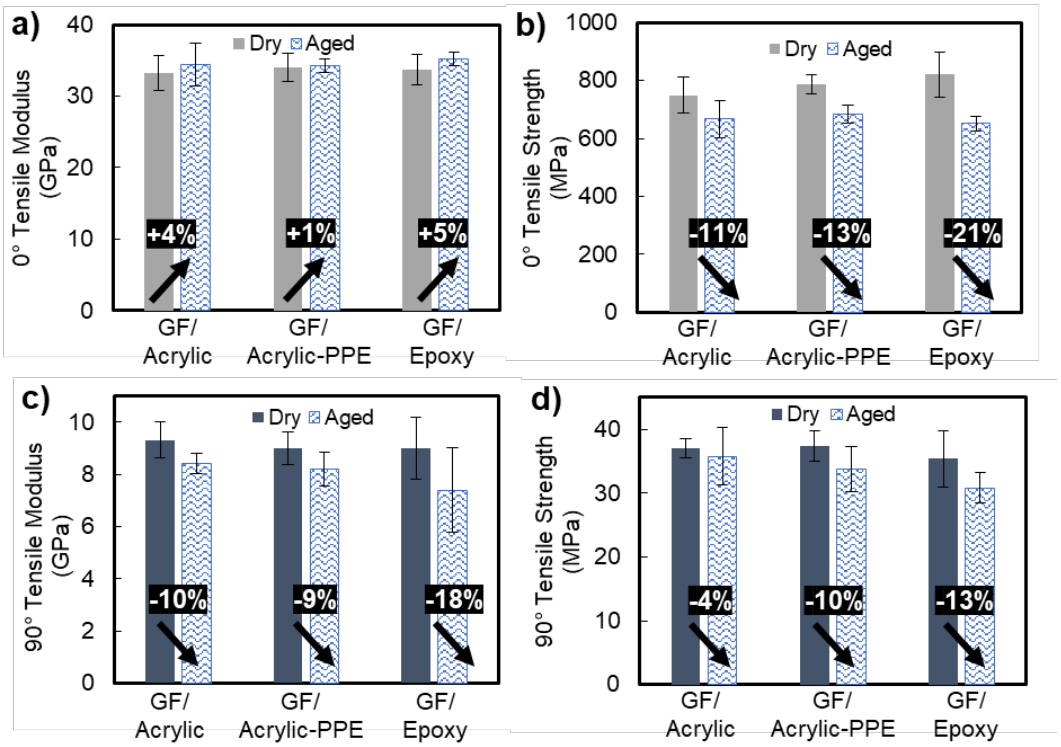


**Figure 4**

As noted in Section 1, a large decrease in strength (-50%) was reported by Davies et al. [14] for 0/90° woven GF/acrylic composites. The differences in fabric weave, sizing agent, resin (Elium® RT300) and ageing conditions (18 months in 80°C seawater) used by the authors may account for this discrepancy from the current results.

### 3.3.3 Flexure

Data from flexural testing is presented in Figure 5. As was observed in the 0° tensile testing, there were no large decreases in 0° flexural modulus as this is a fibre-dominated property. Only the GF/epoxy saw an appreciable decrease of 6% (Figure 5a). The 0° flexural strengths saw larger decreases due to ageing, but there weren't significant differences in the percentage drops between materials, which ranged between 15% and 18%.

In 90° flexure, all three composites were affected by ageing. Reductions in 90° flexural modulus were 17% for GF/acrylic, 13% for GF/acrylic-PPE, and 14% for GF/epoxy (Figure 5c). Even larger drops of 23%, 30% and 22% were observed in the 90° flexural strengths of GF/acrylic, GF/acrylic-PPE, and GF/epoxy respectively (Figure 5d). The GF/epoxy had the highest 90° flexural modulus when dry at 27% higher than GF/acrylic and 18% higher than GF/acrylic-PPE. Similar differences were seen after ageing when GF/epoxy had a 32% higher modulus than GF/acrylic and a 16% higher modulus than GF/acrylic-PPE. This can be attributed to the high degree of crosslinking present in the epoxy matrix adding rigidity.

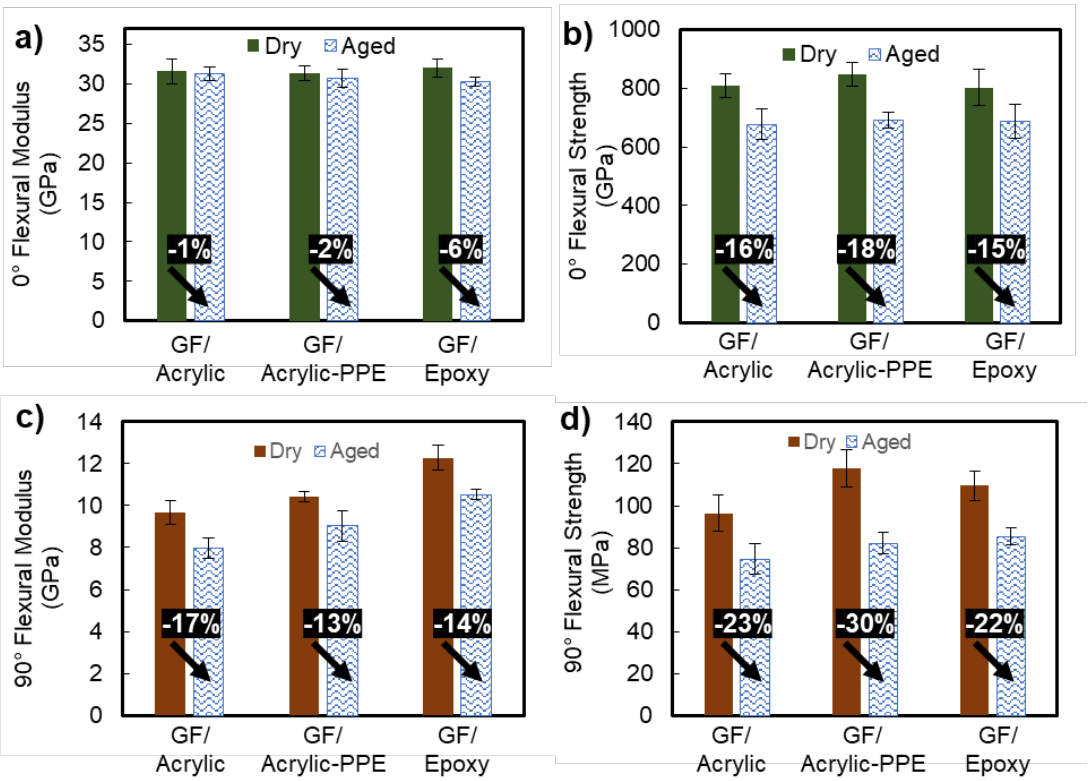


**Figure 5**

Comparing the GF/acrylic and GF/acrylic-PPE, the addition of PPE enhanced 90° flexural properties. GF/acrylic-PPE had an 8% higher modulus when dry and a 13% higher modulus when aged (Figure 5c). Strength was increased by 22% when dry and 10% when aged (Figure 5d). The localised crosslinked regions in the acrylic-PPE matrix therefore have a similar effect to the crosslinking in epoxy, increasing both strength and modulus, but thermoplasticity is retained as acrylic-PPE resin coupons can be reshaped upon heating [15].

### 3.3.4 Short Beam Strength

The short beam strength (Figure 6) of GF/acrylic and GF/acrylic-PPE were equivalent when dry and 28% higher than GF/epoxy. During water ageing, however, GF/acrylic and GF/acrylic-PPE saw larger drops of approximately 30% vs. 13% for GF/epoxy. The strengths after ageing were equivalent for the three materials. The higher drop in SBS in the GF/acrylic and GF/acrylic-PPE can be attributed to both the plasticisation of the matrix and weakening of the fibre/matrix interface [12]. SEM investigations, however, revealed that interfacial debonding during failure played a dominant role, as reported in Section 3.4.

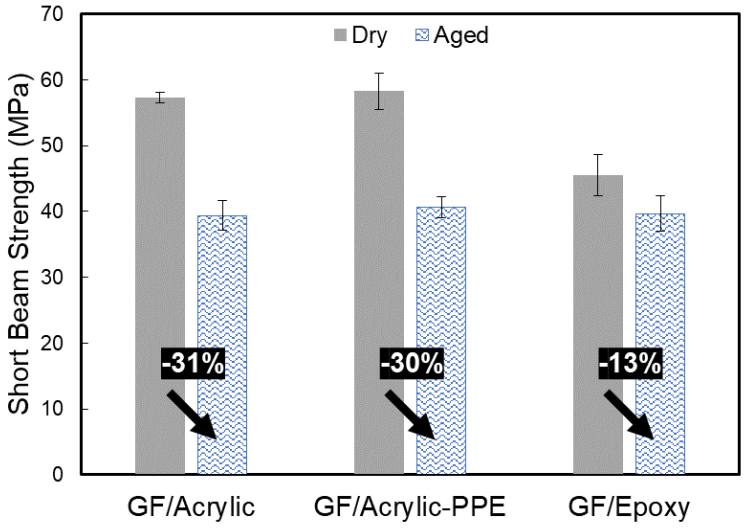


**Figure 6**

### 3.4 SEM and Fracture

In this section, the reasons for the observed differences in mechanical properties caused by ageing are explored using SEM. The 0° tensile specimens of all matrices, both dry and aged, failed via longitudinal splitting or *brooming*. The differences in crack propagation between the composites were determined via SEM imaging of failed 0° tensile specimens as shown schematically in Figure S7. Representative images of 0° tensile fracture surfaces of dry and aged composites are compared in Figure 7.

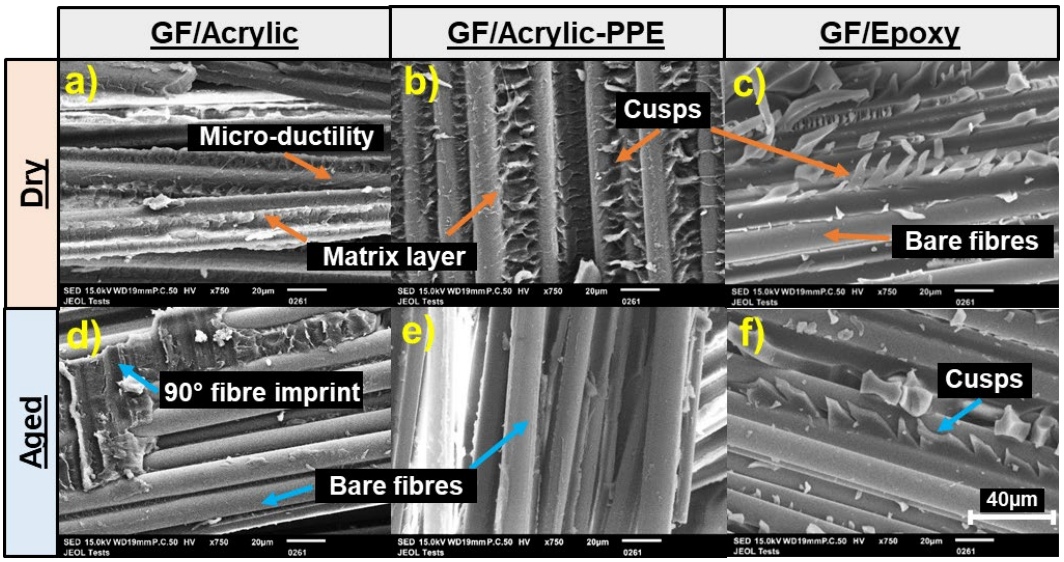


**Figure 7**

### 3.4.1 GF/Acrylic and GF/Acrylic-PPE

The images of GF/acrylic and GF/acrylic-PPE show similar fracture behaviour. In the dry state, there is a matrix layer covering the fibres after fracture (Figures 7a and b). Evidence of the microductility of the thermoplastic matrices is also seen in Figures 7a and b, as are cusps, which are formed by shear failure during longitudinal splitting. After ageing, however, the fibres appear bare, devoid of any adhered matrix layer.

This difference in behaviour can be explained through the Cook-Gordon mechanism [30-34], which describes the propagation of a crack through an anisotropic, inhomogeneous material as it reaches a weak plane—in this case, the fibre-matrix interface. Immediately at the crack tip in 0° tensile testing, the 0° tensile stress ($\sigma_1$) is at a maximum. In addition, shear ($\tau$) and transverse tensile ($\sigma_2$) stresses are present, the latter of which reaches a maximum ahead of the crack tip. If the interface is weak relative to the matrix, $\sigma_2$ causes interfacial debonding ahead of the crack tip, and the crack propagates along the interface (adhesive failure in Figure 8). If the interface is strong, shear forces cause longitudinal splitting through the matrix, parallel to the fibres, and the formation of shear cusps (cohesive failure in Figure 8) [35].

Cohesive failure was detected in the dry GF/acrylic and GF/acrylic-PPE specimens (Figures 7a and b) whereas adhesive failure was detected in the aged GF/acrylic, the aged GF/acrylic-PPE and both dry and aged GF/epoxy specimens (Figure 7c-f). The GF/acrylic and GF/acrylic-PPE therefore have a strong interface when dry and a weak interface after ageing. This switch from cohesive to adhesive failure in GF/acrylic and GF/acrylic-PPE suggests the weakening of the interface must be more significant than any weakening of the acrylic and acrylic-PPE matrices from plasticisation. This is confirmed by the large drops in SBS measured in these specimens (Figure 6).

The reduction in interfacial strength can be attributed to the hydrolysis of the sizing agent which, although proprietary, can be assumed to contain a silane coupling agent which is typical for glass-fibre composites [36]. The bond formed between the coupling agent and the GF is easily hydrolysed; for example, silane sizings can be removed from GF by simply boiling in water [36, 37]. As depicted in Figure 9, sizing hydrolysis in combination with matrix swelling causes debonding of the matrix from the fibres and therefore leads to interfacial degradation as observed in this study.

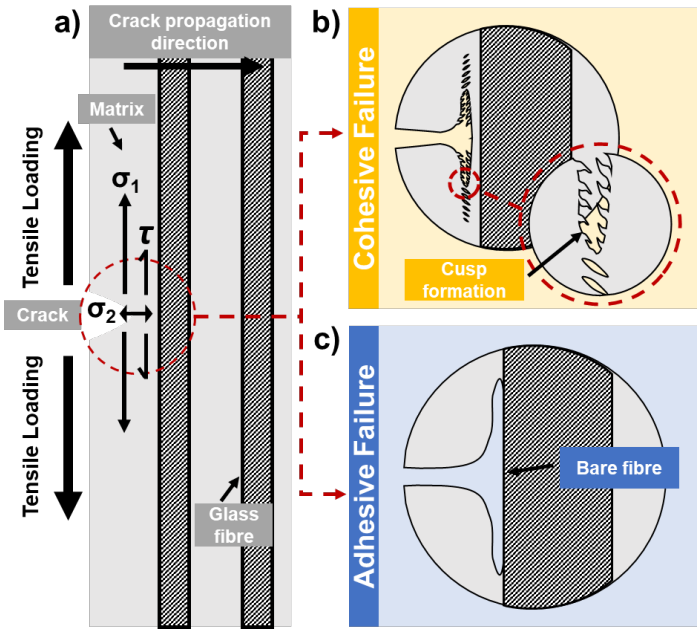


**Figure 8**

### 3.4.2 GF/Epoxy

The SEM images in Figure 7 show different failure behaviour between the thermoplastic composites and the thermoset GF/epoxy. In the former, crack propagation is through the matrix (cohesive failure) when dry but along the interface (adhesive failure) when aged. In contrast, crack propagation is along the interface in both dry and aged epoxy. This may indicate that the crosslinked epoxy matrix is stronger than the epoxy-GF interface both before and after ageing. This is likely, given that it is a crosslinked thermoset matrix rather than an amorphous thermoplastic like acrylic.

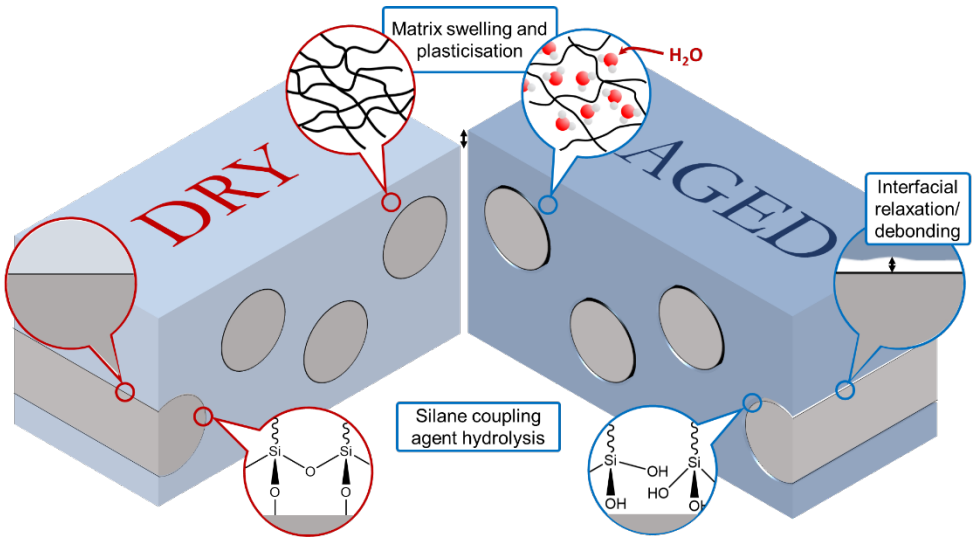


**Figure 9**

# 4 Conclusions

This study aimed to determine the behaviour of thermoplastic GF/acrylic and GF/acrylic-PPE composites during and after ageing in seawater at 50°C, in comparison with an equivalent thermoset GF/epoxy composite.

The diffusion coefficients of the GF/acrylic ($1.8\times10^{-12}$ $m^2$ $s^{-1}$) and GF/acrylic-PPE ($3.4\times10^{-12}$ $m^2$ $s^{-1}$) were an order of magnitude larger than that of GF/epoxy ($0.16\times10^{-12}$ $m^2$ $s^{-1}$), and the final masses of absorbed water in GF/acrylic and GF/acrylic-PPE were also higher at 0.91% and 0.81% vs. 0.63% for GF/epoxy, respectively. This difference is likely due to a combination of higher void contents in the thermoplastic composite coupons used for water diffusion studies and a stronger interaction of the epoxy matrix with water in GF/epoxy. The faster water diffusion in the thermoplastic composites, however, did not correspond to greater reductions in mechanical properties due to ageing. In general, the GF/acrylic and GF/acrylic-PPE compared favourably and had similar or smaller reductions in mechanical properties due to seawater ageing compared to the GF/epoxy baseline. The effect of free water in voids and interstitial sites may therefore be less detrimental than bound water.

The 0° tensile and flexural moduli were approximately equal between matrices and not significantly affected by ageing. The strengths, however, saw larger decreases—up to 20% in the case of GF/epoxy in 0° tension. SEM imaging of these specimens, along with DMA studies, reveal that interfacial degradation and matrix plasticisation are the causes of deterioration in mechanical properties after seawater ageing. Future studies may therefore focus on determining the effects of acrylic-tailored sizings on the degradation of GF/acrylic composites in water.

The most significant mechanical benefits of GF/acrylic-PPE over GF/acrylic were found in 90° flexural testing. GF/acrylic-PPE had higher 90° flexural strength (+22%) and modulus (+8%) when dry, and also enhanced 90° flexural strength (+10%) and modulus (+13%) when aged, compared to GF/acrylic. In addition, the $T_g$ of the GF/acrylic-PPE was 4°C higher than the GF/acrylic before ageing and 6°C after ageing. DMA revealed no evidence of melt-softening behaviour by 180°C in the GF/acrylic-PPE, whereas the onset of softening was observed in GF/acrylic.

These results add further evidence that thermoplastic acrylic composites are a promising recyclable alternative to thermosets in marine applications, given their favourable material properties when

compared to an epoxy baseline. In addition, acrylic-PPE allows for improved mechanical and thermomechanical properties while remaining recyclable.

## 5 Acknowledgements

The authors are grateful for funding provided by the Wind and Marine Energy Systems and Structures Centre for Doctoral Training (WAMESS CDT) and to Prof Andy Mount Dean of Research at CSE UoE and EPSRC IAA support team at Edinburgh Innovations. The authors gratefully acknowledge Arkema GRL, France and SABIC for the provision of materials towards this research. SABIC and brands marked with ™ are trademarks of SABIC or its subsidiaries or affiliates unless otherwise noted.

## 6 References

[1] Liu P, Barlow CY. Wind turbine blade waste in 2050. Waste Management. 2017;62:229-40.

[2] IEA. Net Zero by 2050 A Roadmap for the Global Energy Sector. 2021.

[3] Nash NH, Portela A, Bachour-Sirerol CI, Manolakis I, Comer AJ. Effect of environmental conditioning on the properties of thermosetting- and thermoplastic-matrix composite materials by resin infusion for marine applications. Composites Part B: Engineering. 2019;177.

[4] Qin Y, Summerscales J, Graham-Jones J, Meng M, Pemberton R. Monomer Selection for In Situ Polymerization Infusion Manufacture of Natural-Fiber Reinforced Thermoplastic-Matrix Marine Composites. Polymers. 2020;12(12).

[5] Cousins DS, Suzuki Y, Murray RE, Samaniuk JR, Stebner AP. Recycling glass fiber thermoplastic composites from wind turbine blades. Journal of Cleaner Production. 2019;209:1252-63.

[6] Gebhardt M, Manolakis I, Chatterjee A, Kalinka G, Deubener J, Pfnür H, et al. Reducing the raw material usage for room temperature infusible and polymerisable thermoplastic CFRPs through reuse of recycled waste matrix material. Composites Part B: Engineering. 2021;216.

[7] Meyer Zu Reckendorf I, Sahki A, Perrin D, Lacoste C, Bergeret A, Ohayon A, et al. Chemical Recycling of Vacuum-Infused Thermoplastic Acrylate-Based Composites Reinforced by Basalt Fabrics. Polymers (Basel). 2022;14(6).

[8] Bel Haj Frej H, Léger R, Perrin D, Ienny P, Gérard P, Devaux J-F. Recovery and reuse of carbon fibre and acrylic resin from thermoplastic composites used in marine application. Resources, Conservation and Recycling. 2021;173.

[9] Obande W, Stankovic D, Bajpai A, Devine M, Wurzer C, Lykkeberg A, et al. Thermal reshaping as a route for reuse of end-of-life glass fibre-reinforced acrylic composites. Composites Part B: Engineering. 2023;257.

[10] Obande W, Mamalis D, Ray D, Yang L, Ó Brádaigh CM. Mechanical and thermomechanical characterisation of vacuum-infused thermoplastic- and thermoset-based composites. Materials & Design. 2019;175.

[11] Davies P, Arhant M. Fatigue Behaviour of Acrylic Matrix Composites: Influence of Seawater. Applied Composite Materials. 2018;26(2):507-18.

[12] Bel Haj Frej H, Léger R, Perrin D, Ienny P. A Novel Thermoplastic Composite for Marine Applications: Comparison of the Effects of Aging on Mechanical Properties and Diffusion Mechanisms. Applied Composite Materials. 2021.

[13] Barbosa LCM, Santos M, Oliveira TLL, Gomes GF, Ancelotti Junior AC. Effects of moisture absorption on mechanical and viscoelastic properties in liquid thermoplastic resin/carbon fiber composites. Polymer Engineering & Science. 2019;59(11):2185-94.

[14] Davies P, Le Gac PY, Le Gall M. Influence of Sea Water Aging on the Mechanical Behaviour of Acrylic Matrix Composites. Applied Composite Materials. 2016;24(1):97-111.

[15] Obande W, Gruszka W, Garden JA, Wurzer C, Ó Brádaigh CM, Ray D. Enhancing the solvent resistance and thermomechanical properties of thermoplastic acrylic polymers and composites via reactive hybridisation. Materials & Design. 2021;206.

[16] Obande W, Ó Brádaigh CM, Ray D. Thermoplastic hybrid-matrix composite prepared by a room-temperature vacuum infusion and in-situ polymerisation process. Composites Communications. 2020;22(August):22-7.

[17] Unemori M, Matsuya Y, Matsuya S, Akashi A, Akamine A. Water absorption of poly(methyl methacrylate) containing 4-methacryloxyethyl trimellitic anhydride. Biomaterials. 2003;24(8):1381-7.

[18] Moghbelli E, Banyay R, Sue H-J. Effect of moisture exposure on scratch resistance of PMMA. Tribology International. 2014;69:46-51.

[19] Tsenoglou CJ, Pavlidou S, Papaspyrides CD. Evaluation of interfacial relaxation due to water absorption in fiber–polymer composites. Composites Science and Technology. 2006;66(15):2855-64.

[20] Fujii Y, Tominaga T, Murakami D, Tanaka M, Seto H. Local Dynamics of the Hydration Water and Poly(Methyl Methacrylate) Chains in PMMA Networks. Front Chem. 2021;9:728738.

[21] Abdelmola F, Carlsson LA. State of water in void-free and void-containing epoxy specimens. J Reinf Plast Compos. 2019;38(12):556-66.

[22] Bellenger V, Verdu J, Morel E. Structure-properties relationships for densely cross-linked epoxide-amine systems based on epoxide or amine mixtures. Journal of Materials Science. 1989;24(1):63-8.

[23] Thominette F, Gaudichet-Maurin E, Verdu J. Effect of Structure on Water Diffusion in Hydrophilic Polymers. Defect and Diffusion Forum. 2006;258-260:442 - 6.

[24] Bel Haj Frej H, Léger R, Perrin D, Ienny P. Effect of aging temperature on a thermoset-like novel acrylic thermoplastic composite for marine vessels. Journal of Composite Materials. 2021;55(19):2673-91.

[25] Bond DA, Smith PA. Modeling the Transport of Low-Molecular-Weight Penetrants Within Polymer Matrix Composites. Applied Mechanics Reviews. 2006;59(5):249-68.

[26] Smith LSA, Schmitz V. The effect of water on the glass transition temperature of poly(methyl methacrylate). Polymer. 1988;29(10):1871-8.

[27] Wright WW. The effect of diffusion of water into epoxy resins and their carbon-fibre reinforced composites. Composites. 1981;12(3):201-5.

[28] Chateauminois A, Chabert B, Soulier JP, Vincent L. Dynamic mechanical analysis of epoxy composites plasticized by water: Artifact and reality. Polym Compos. 1995;16(4):288-96.

[29] Joseph P, Tretsiakova-McNally S. Melt-Flow Behaviours of Thermoplastic Materials under Fire Conditions: Recent Experimental Studies and Some Theoretical Approaches. Materials (Basel). 2015;8(12):8793-803.

[30] Cook J, Gordon JE. A mechanism for the control of crack propagation in all-brittle systems. Proceedings of the Royal Society of London Series A Mathematical and Physical Sciences. 1964;282(1391):508-20.

[31] Ma Y, Yang Y, Sugahara T, Hamada H. A study on the failure behavior and mechanical properties of unidirectional fiber reinforced thermosetting and thermoplastic composites. Composites Part B: Engineering. 2016;99:162-72.

[32] Thouless M, Parmigiani J. Mixed-mode cohesive-zone models for delamination and deflection in composites. Proceedings of the 28th Risø International Symposium on Material Science: Interface Design of Polymer matrix Composites. 2007.

[33] Raab M, Schulz E, Sova M. The cook-gordon mechanism in polymeric materials. Polymer Engineering & Science. 1993;33(21):1438-43.

[34] Fibre-dominated failures of polymer composites. In: Greenhalgh ES, editor. Failure Analysis and Fractography of Polymer Composites: Woodhead Publishing; 2009. p. 107-63.

[35] Delamination-dominated failures in polymer composites. In: Greenhalgh ES, editor. Failure Analysis and Fractography of Polymer Composites: Woodhead Publishing; 2009. p. 164-237.

[36] Thomason JL. Glass fibre sizing: A review. Composites Part A: Applied Science and Manufacturing. 2019;127.

[37] Ishai O. Environmental effects on deformation, strength, and degradation of unidirectional glass-fiber reinforced plastics. II. Experimental study. Polymer Engineering & Science. 1975;15(7):491-9.

[38] Nihei T. Dental applications for silane coupling agents. J Oral Sci. 2016;58(2):151-5.

## 7 Figure Captions

**Figure 1:** The water absorption curves of the three composites with their corresponding void volume fractions. The experimental data are presented as points and the fitted Fickian diffusion curves as dotted lines. A decrease in the diffusion coefficient is visible in the GF/epoxy after approximately 4 days.

**Figure 2:** A comparison of the polymer and composite structures as relevant to the diffusion of water. (a) Acrylic polymer with (i) polar carbonyl groups with the acrylic chains and (ii) free volume. (b) Acrylic-PPE with (i) carbonyl groups in the acrylic chains, (ii) free volume and (iii) PPE oligomers with methacrylate end groups highlighted in red. (c) Epoxy has (i) hydroxyl groups and (ii) amine groups from the hardener.

**Figure 3:** (Top) The $T_g$ of GF/acrylic, GF/acrylic-PPE and GF/epoxy before and after ageing as determined via DMA. (Bottom) Tan δ vs. temperature for the dry (solid lines) and aged (dotted lines) coupons. In the aged specimens, a shoulder or secondary peak is present due to drying. Flow behaviour of the acrylic matrix in the dry and aged GF/acrylic is highlighted (curves 1 and 2).

**Figure 4:** The tensile properties of the composites are displayed before and after ageing with percentage changes. The 0° tensile properties are normalised to 50% FVF and *found in (a) and (b). T*he 90° tensile properties *are* in (c) and (d). All error bars are ±1 standard deviation.

**Figure 5:** The flexural properties of the composites are displayed before and after ageing with percentage changes. The 0° flexural properties are normalised to 50% FVF and are found in (a) and (b). *T*he 90° flexural properties *are* in (c) and (d).

**Figure 6:** The SBS of the composites when dry (grey) and aged (blue). The percentage drop in strength due to ageing is highlighted.

**Figure 7:** SEM images of 0° tension specimen fracture surfaces with fractographic features annotated.

**Figure 8:** Fracture propagation under 0° tension with 0° tensile stress ($\sigma_1$), 90° tensile stress ($\sigma_2$) and shear stress ($\tau$) ahead of the crack tip labelled [30]. Cohesive failure indicates a strong interface and adhesive failure indicates a weak interface relative to the matrix.

**Figure 9:** A comparison of dry (left) and seawater aged (right) composites demonstrating some damage mechanisms of seawater ageing [25, 38].

## 8 Table Captions

**Table 1:** The diffusion coefficients measured in this study along with values from literature for comparison.

**Table 2:** Fibre and void volume fractions of composites used for mechanical testing.